Refined tip preparation by electrochemical etching and ultrahigh vacuum treatment to obtain atomically sharp tips for scanning tunneling microscope and atomic force microscope

Till Hagedorn,[a] Mehdi El Ouali, William Paul, David Oliver,
Yoichi Miyahara, and Peter Grütter[b]
Department of Physics, McGill University, 3600 Rue University, Montreal, QC H3A2T8, Canada

(Received 17 July 2011; accepted 17 October 2011; published online 29 November 2011)

A modification of the common electrochemical etching setup is presented. The described method reproducibly yields sharp tungsten tips for usage in the scanning tunneling microscope and tuning fork atomic force microscope. *In situ* treatment under ultrahigh vacuum ($p \leq 10^{-10}$ mbar) conditions for cleaning and fine sharpening with minimal blunting is described. The structure of the microscopic apex of these tips is atomically resolved with field ion microscopy and cross checked with field emission. © *2011 American Institute of Physics*. [doi:10.1063/1.3660279]

I. INTRODUCTION

In all scanning probe microscopy (SPM) methods, the tip that probes the sample plays a key role in understanding the results.[1,2] Tip preparation and characterization is therefore vital for a physically meaningful interpretation of SPM results. In scanning tunneling microscopy (STM) most researchers use tips that are electrochemically etched from cold-drawn polycrystalline tungsten wire.[2] More and more researchers use quartz tuning forks with attached tungsten tips for atomic force microscopy (AFM) like the q-plus sensor.[3] These tips are also electrochemically etched. Therefore, the desire for a reliable tip etching method is great. Many different methods have been developed. This article presents a modified version of the *drop-off* technique described by Ibe *et al.*[4] and further developed by other authors such as Melmed *et al.*[5] Lately, the lamella technique[6] has become more popular. Another 3 step process using the *drop-off* technique has been proposed recently.[7] This 3 step technique allows a fine tuning of the tip shape and produces tips with radii of about 3 nm before *in situ* heating in UHV. The work presented in this paper, focuses on the traditional *drop-off* method and shows how well the electrochemical etching works once the liquid cell is divided into a tip part and a counter electrode part with a large opening for the ion current. The etching process is monitored and traces of the etching current versus time are given. Field emission (in the form of Fowler-Nordheim plots) is used as *in situ* sharpness test after resistive heating cycles. Finally, atomically resolved field ion microscopy (FIM) images[8,9] are presented. By analyzing the FIM images it is shown that the presented method produces tips with a radius of about 3–15 nm after *in situ* UHV cleaning in a highly reproducible way. Besides the small tip radius, these tips have a clean tip surface and can be further prepared by controlled indentation into the sample material for high resolution STM and AFM imaging and spectroscopy.

[a]Electronic mail: hagedorn@physics.mcgill.ca.
[b]Electronic mail: grutter@physics.mcgill.ca.

II. ELECTROCHEMICAL ETCHING OF TUNGSTEN

Figure 1(a) shows the electrochemical tip etching setup. The wire that one wants to etch is dipped into an electrolyte solution that etches the wire at point A (*dip-in* length 0.65 mm – defined as the distance that the wire is introduced in the solution after the liquid makes contact with the wire). The *dip-in* length is critical and has to be found for each setup, concentration and wire diameter as further discussed in Ref. 7. A micrometer screw (F) is used to realize and to measure the vertical motion. A counter electrode (D) is immersed in the solution as well. This electrode is a loop of stainless steel wire with a wire diameter of 0.55 mm. The power is supplied by a dc power supply (E), which has a differentiator circuit inside. This differentiator ensures the quick switch-off of the etching bias voltage to prevent blunting by etching after the *drop-off*. The whole setup is placed on a large steel plate that has a foam layer underneath. This isolates the system from mechanical vibrations.

Once the power is switched on, a constant voltage of 3.0 V is applied (tip on positive bias) and the well-known etching reaction

$$\mathrm{W(solid)} + 2\,\mathrm{OH^-} + 2\,\mathrm{H_2O} \rightarrow \mathrm{WO_4^{2-}} + 3\,\mathrm{H_2(gas)} \qquad (1)$$

starts.[4] Details about the oxidation steps can be found in Ref. 10. Potassium hydroxide (KOH) in DI-water is used in our case as etching solution ($c \sim 9.85$ mol/l). A crucial difference between the setup presented here and most of the setups using a divided liquid cell that have been published[4,5,11] is that a glass cylinder with a large diameter (21.0 mm) compared to the wire diameter (0.100–0.127 mm) is used. This ensures a good ion current flow (C in Figure 1(a)) and minimum disturbance due to turbulence around the meniscus (A in Figure 1(a)). A photo of the setup is shown in Figure 1(b).

As the etching progresses the wire becomes very thin at the meniscus and the bottom part of the wire breaks off due to gravity. This produces a tip that has only a few atoms at the point of rupture.[7–9] In order to stop the etching right after the *drop-off* and prevent blunting due to further etching, the power supply has to switch off just after the wire breaks.

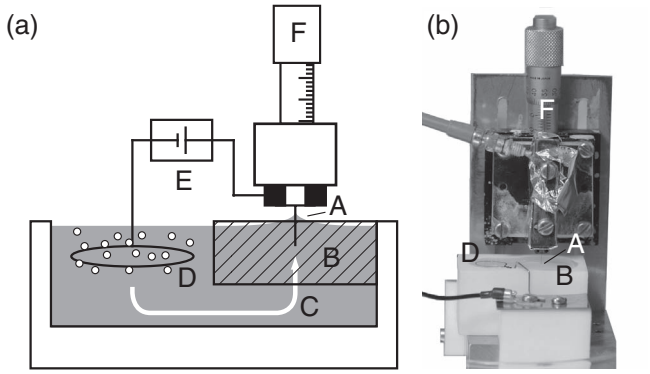

FIG. 1. (a) The tip etching setup. In this configuration the meniscus region (A), where the wire gets etched, is shielded from the cathode (D) by a glass cylinder (B). This leads to a mechanical isolation of the liquid surface from the hydrogen bubbles that build up at the cathode. (b) A photo of the tip etching setup.

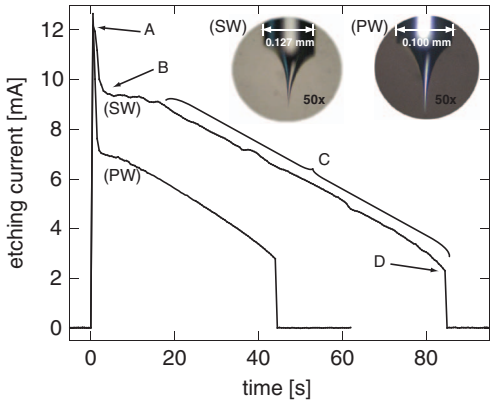

FIG. 3. (Color online) Etching current versus time shown for a single crystalline tungsten wire (SW) and for a polycrystalline wire (PW). The insets show optical microscopy images (magnification 50×) of the corresponding tips.

Descriptions of suitable power supply designs can be found in the literature.[4,12,13]

A technical drawing of the container is shown in Figure 2. It is a block of teflon that is 26.0 mm wide, 44.0 mm long, and 23.0 mm high. A 37.0 mm long and 17.0 mm deep slot is milled (17.0 mm diameter end mill) first into the material. Then a hole (37.0 mm diameter) is drilled 9.0 mm deep at one end to hold the glass cylinder as indicated in Figure 2. The exact measurements are not critical and can be adjusted to any available glass cylinder of similar dimensions. The glass cylinder is cut from a cylindrical storage container.

To have a better understanding of the stability of the etching process, the etching current is recorded. Two traces of the etching current vs. time can be found in Figure 3 for a single crystalline tungsten wire (SW) ((111) orientation) and a polycrystalline tungsten wire (PW). The graphs show a spike at the beginning (A) (12.2 mA for SW and 12.6 mA for PW) and after 1.5–3 s the process stabilizes (B) (9.4 mA for SW and 7.0 mA for PW). The spike originates from the fact that the bottom part of the wire is bare at the beginning and OH^- ions can reach the whole bottom part. As the etching progresses the bottom part of the wire will be covered with WO_4^{2-} and mainly the meniscus region contributes to the current. Therefore, the current decreases quickly back to a more stable value. Then the current decreases almost linearly (C) (the slope for both traces is $s = -0.1$ mA/s) until the bottom part drops off (D) (at 2.3 mA for SW and 2.8 mA for PW). The *drop-off* current and the etching time is very reproducible for a given concentration, counter electrode cleanliness, and wire diameter. Compared to other methods a rather high concentration (9–10 mol/l) is used here and therefore the etching time is very short (84.0 s for SW and 43.0 s for PW for the shown traces; the difference in the etching time for the SW and PW traces is due to the different wire diameter – see Table II for average values of the etching time).

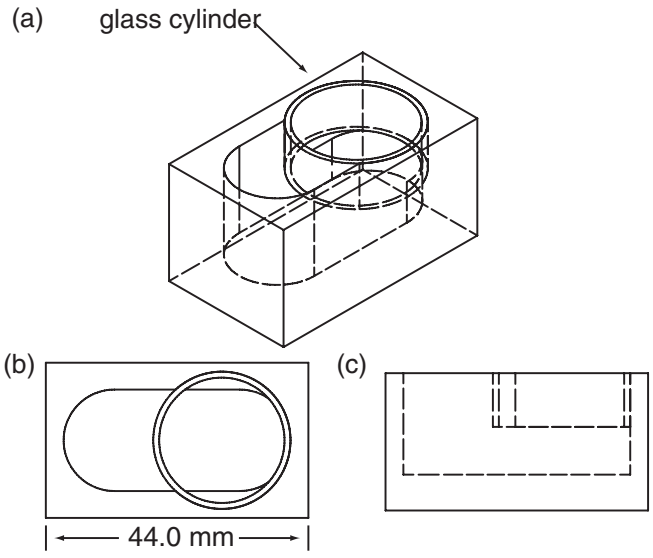

FIG. 2. (a) Isometric view of the container with inserted glass cylinder to show the internal structure. (b) Top view drawing of the etching container with inserted glass cylinder. (c) Side view of the container.

Right after the *drop-off* the tip is retracted, cleaned with a DI-water, ethanol, acetone, and ethanol sequence to remove etching residues and the macroscopic shape is checked in an optical microscope (insets (SW) and (PW) in Figure 3). At this point it is useful to point out an advantage of this method over the lamella technique.[6] The wire can be pre-etched with the *drop-off* technique which leads to reduced surface roughness in the meniscus region at the start of the tip etching, leading to a more defined tip shank. Another advantage is the small amount of wire that is used which is important when working with expensive single crystalline wires (200 $/cm).

A. Troubleshooting

The following disturbances have to be eliminated in order to obtain similar results to what is presented here.

- Flakes from the PW wire surface by pre-etching.
- Air turbulences (e.g., building ventilation or people passing by) disturb the liquid surface. As consequence of the oscillating liquid surface the etching current will show a 1–5 Hz modulation.

- Fibers on the liquid surface might force the meniscus to drop. As a consequence a sharp drop in the etching current will cause the electronics to switch off before the *drop-off*.
- A large tilt of the wire will result in an undefined *drop-off* and should be avoided.
- Air bubbles at the wire surface will move up the wire surface and cause severe disturbances – pre-etching helps to reduce the roughness of the wire's surface and the chance of producing these small bubbles during the dipping process is reduced.

III. *IN SITU* TIP CLEANING AND CHARACTERIZATION

A. Resistive heating

It is a well-known fact that several contaminations are left on the tungsten surface after the electrochemical etching besides the native oxide layer that forms on tungsten under atmospheric conditions. Therefore, a number of oxides (mainly in the form of WO_3) and residues of KOH are present.[14] Heating the tungsten tip surface to temperatures above 1075 K in UHV causes the following reaction:

$$2\,WO_3 + W \rightarrow 3\,WO_2 \uparrow . \qquad (2)$$

This process sublimes the oxide layer along with other contaminations[2,8] and thermal diffusion heals structural imperfections. Since a conductive and stable tip is needed for STM operation, these effects are advantageous. The tip sits at the end of a spot welded wire T-cross as seen in the inset (i) of Figure 4. Running a current through the wire base resistively heats the tip. Before heating to high temperatures (flash heating) a current of 2 A with a voltage of about 1.5 V is applied for about 5 min in UHV. This degasses the tip and pre-cleans it from etching residues and air contaminates.[15] Finally, the voltage is increased slowly (about 15–30 s from the degassing voltage to the voltage needed for red glow) until the red glow of the T-cross is observed. The power is left constant for 3–5 s and then reduced and switched off (the voltage reduction can be fast).

The voltage is controlled during the heating process and therefore the dissipated power is limited as one can see from $P(V) = V^2/R$. The voltage is controlled and constant unless changed by the user. But the resistance of a metal wire increases with increasing temperature. Therefore, the power is limited when controlling the voltage (if the current was controlled, the dissipated power could increase with increased resistance since $P(I) = I^2 R$). This is important since a rapid increase in the heating power could easily blunt the tip.[16] A change in the resistance of the spot welding contacts during the resistive heating can also lead to a spike in the heating power. This has to be expected for the first heating cycle after the tip is introduced into UHV in our setup.

Resistive heating is a useful tool since it cleans the whole tungsten wire. Local heating, like electron bombardment, cleans the tip only in the apex region and increases the chance that residues from the tip shank diffuse towards the tip apex during the STM measurement. Examples of blunted tips and a comparison of different tip cleaning methods can be found in Ref. 11. In our case the actual voltage and current values for the flash heating vary from tip to tip since the resistance is different for different spot welding contacts. Therefore, a visual check is the most reliable control of the process. Mostly a current of about 2.5–3.0 A at about 3–4 V is used, like shown in the inset (i) in Figure 4.

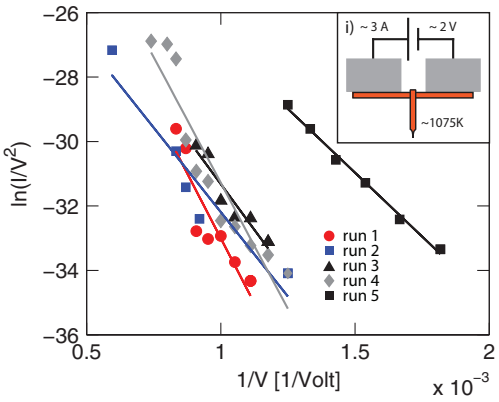

FIG. 4. (Color online) Fowler-Nordheim plots of a series of five consecutive runs of resistive heating/ field emission cycles for a single crystalline tungsten tip (W(111)). The result is a clean and sharp tip (run 5 – smaller slope) that field emits at lower applied voltages (higher 1/V values) than the initial run (run 1). Inset (i) shows the wire T-cross and the circuit for the resistive heating of the tip.

B. Field emission

Field emission measurements are a well-known method to check the tip radius as well as the surface cleanliness and structural stability of the tip. The background for this method can be found in Ref. 8. Using the Fowler-Nordheim theory of cold field emission from a metal tip,[17] one obtains

$$\ln\left(\frac{I}{V^2}\right) = \underbrace{\ln\left(a\,6.2\times10^{-6}\frac{(\mu/\phi)^{1/2}}{\alpha^2(\mu+\phi)(kR)^2}\right)}_{\text{offset}} - \underbrace{6.8\,\phi^{3/2}\alpha k R}_{\text{slope}}\cdot\frac{1}{V},$$

where I is the emission current (in nA), V is the applied voltage (in V), a is the field emitting region (in cm), μ is the Fermi energy (in eV), ϕ is the workfunction (in eV), α is a correction parameter, k is a geometric tip factor, and R is the tip radius (in nm).

The field emission data is plotted as $\ln(I/V^2)$ vs. 1/V in a so-called Fowler-Nordheim plot. Using an average work function value of $\phi = 4.5$ eV for tungsten and $\alpha = 1$ (which is justified in Ref. 18), the slope of the resulting graph yields kR. Since the factor k is assumed to be between 5 and 35, [18] one can compute R_{min} from this method ($R_{min} = kR/35$).

An example of Fowler-Nordheim plots can be found in Figure 4. A disc made out of oxygen-free copper at a distance of about 2.5 cm from the tip is used as the counter electrode for our field emission measurements. Different field emission runs are shown for the same tip – the results obtained for kR

TABLE I. Results for field emission measurements shown in Figure 4.

Run	kR (nm)	R_{min} (nm)
1	248	7
2	162	5
3	174	5
4	241	7
5	122	3

and R_{min} from the fitting procedure are given in Table I. The main point here is that the tip sharpness can be judged by the slope – a smaller radius indicates a smaller slope as seen in run 5 versus the runs recorded before.

C. Resistive heating/field emission cycles

Figure 4 shows a set of field emission curves of a single crystalline tip (W(111)) plotted as a Fowler-Nordheim plot.[8] A cycle of several combined field emission and heating runs is shown. It is necessary to do several runs since good tip properties are rarely achieved in the first run. The exact procedure for the 5 curves is:

1. flash heating for 3 s,
2. field emission run 1 (up to 1.2 kV),
3. flash heating for 3 s,
4. field emission runs 2 (up to 1.7 kV) and 3 (up to 1.1 kV), and
5. field emission runs 4 (up to 1.4 kV) and 5 (up to 0.8 kV) one day later.

High applied fields, as used in runs 2, 3, and 4, improve the tip structure in many different ways. The field enhancement at the tip apex is great and therefore diffusion is enhanced which leads to an overall smoother tip and might build well structured tip apexes as shown in Ref. 19. Field evaporation of tungsten oxide that was not cleaned by resistive heating during the field emission characterization is another process which further cleans the tip.[8] A reduced scattering of the data in run 5 signifies a smooth and clean tip surface.

The field emission measurements are a good estimate of the tip radius, structural stability, and surface cleanliness using reference values. Our field ion microscope (FIM) can only image very sharp tips with a radius of 3–15 nm. From experience we know that tips that are suitable for our FIM setup show an emission current of $I \geq 10$ nA at $V \leq 1300$ V.

D. Field ion microscopy

As described in Refs. 8, 18, 20, and 21, FIM enables the experimenter to acquire atomically resolved images of metallic tips. Figure 5(a) shows an example of a FIM image of a single crystalline tip that was prepared as described above. The orientation of the tip apex is along the [111] direction. Not all tip atoms are imaged with FIM. Each image spot on the screen in Figure 5(a) relates to an edge atom or a protruded atom. Using a model that was developed by Moore,[22] a ball model can be constructed from this image

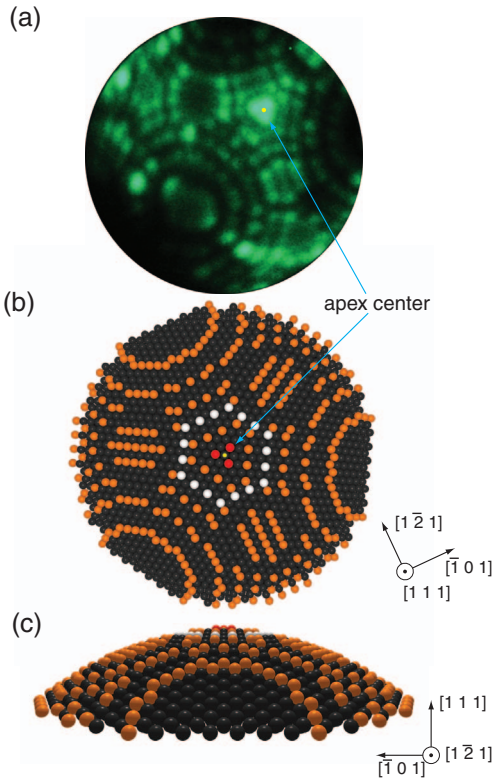

FIG. 5. (Color online) (a) FIM image of a single crystalline tungsten [111] oriented tip at $V_{tip} = 4.8$ kV and room temperature. (b) Top view on the reconstructed ball model with the same orientation as the real FIM picture in (a). (c) Side view of the tip structure. The radius of the reconstructed tip is $r_{tip} = 7.8$ nm.

and accurate information about the atomic tip structure can be obtained. These reconstructions are shown in Figures 5(b) and 5(c). Visible image spots of the FIM image are shown in orange, invisible atoms that complete the structure are shown in black. The apex center is marked with a yellow dot. In order to distinguish the first three layers of the tip, the apex atoms are displayed in red, the second layer edge atoms in orange, and the third layer edge atoms in white. Figure 5(b) shows the top view and Figure 5(c) the side view. For the presented tip a radius of $r_{tip} = 7.8$ nm was evaluated from the ball model and using the ring counting method[8] a radius of $r_{tip} = (7.3 \pm 1.2)$ nm was obtained. Tip indentation experiments have established that the apex of the tip is the part of the tip that touches the surface in a STM experiment.

Single-atom-tips are needed for achieving atomically resolved images in STM and AFM. As discussed in Refs. 8 and 19, FIM can also be used to further refine the tip apex structure by controlled field evaporation into a scratch adhesion test. Another method using adsorbed nitrogen for field assisted sharpening of the STM tip with FIM was developed by Rezeq *et al.*[23] which enables the experimenter to prepare a tip that is terminated by one atom, an additional characterization was given by Fu *et al.*[24] A characterization of thermodynamical stability can be found in Refs. 21 and 25. An investigation of the crystallographic orientation of polycrystalline tungsten wires is given in Ref. 26.

TABLE II. Results for tips that have been characterized with field emission (FE).

Type	$\bar{I}_{drop}$ (mA)	σ_I (mA)	$\bar{t}_{etch}$ (s)	σ_t (s)	FE success
PW	3.5	0.9	49.1	6.9	9/12 = 75 %
SW	4.8	2.2	79.0	9.8	18/20 = 90 %

IV. SUCCESS RATE AND AVERAGE VALUES

As seen in Table II, 32 tips have been etched and FE characterized since switching to this setup. For all etches the *dip-in* length was 0.65 mm and the concentration ranged from 9.78 to 9.95 mol/l. Average values of the *drop-off* current and the etching time for the two different wire types (polycrystalline (PW) and single crystalline (SW) wire) are given. One can see the spread of the data from the standard deviation σ. All of the tips were investigated with field emission. The FE success rate cited in the table shows how many tips reached the threshold that is necessary for FIM. Most of these tips were used for FIM and STM and showed a tip radius between 3 and 15 nm.

A high success rate is very important in our case since all of the *in situ* treatment has several delays, e.g., air lock venting/pumping to bring the tip in and out of the system and the handling inside the vacuum chamber.

V. CONCLUSION

A simple method has been presented that allows well controlled tip etching and *in situ* cleaning. Using this preparation technique tips were prepared that are characterized from the first etching step by recording the etching current, cross-checking the tip shape in an optical microscope, during the heating by controlling the heating power, cross-checking with field emission and finally, just before usage in STM, with FIM by obtaining an atomically resolved image of the tip shape. Tips prepared following this procedure have a radius of 3–15 nm ready to be used in the STM. Sharp STM tips with this radius have been produced before but not in this controlled, reproducible way.

ACKNOWLEDGMENTS

Funding for the project by Natural Sciences and Engineering Research Council (NSERC), FQRNT, and CIfAR is acknowledged. The authors would like to thank Professor Rolf Möller for stimulating discussions regarding the tip structure and its meaning in STM.

[1] W. A. Hofer, A. S. Foster, and A. L. Shluger, Rev. Mod. Phys. **75**, 1287 (2003).
[2] C. J. Chen, *Introduction to Scanning Tunneling Microscopy* (Oxford University Press, New York, 1993).
[3] F. J. Giessibl, Appl. Phys. Lett. **76**, 1470 (2000).
[4] J. P. Ibe, J. P. P. Bey, S. L. Brandow, R. A. Brizzolara, N. A. Burnham, D. P. DiLella, K. P. Lee, C. R. K. Marrian, and R. J. Colton, J. Vac. Sci. Technol. A **8**, 3570 (1990).
[5] A. J. Melmed, in *Fifth International Conference on Scanning Tunneling Microscopy/Spectroscopy* (1991), Vol. 9, pp. 601–608.
[6] M. Kulawik, M. Nowicki, G. Thielsch, L. Cramer, H.-P. Rust, H.-J. Freund, T. P. Pearl, and P. S. Weiss, Rev. Sci. Instrum. **74**, 1027 (2003).
[7] Z. Q. Yu, C. M. Wang, Y. Du, S. Thevuthasan, and I. Lyubinetsky, Ultramicroscopy **108**, 873 (2008).
[8] A.-S. Lucier, H. Mortensen, Y. Sun, and P. Grutter, Phys. Rev. B **72**, 235420 (2005).
[9] A.-S. Lucier, M.S. thesis, McGill University, 3600 Rue University, Montreal, QC H3A 2T8, Canada, 2004).
[10] J. W. Johnson and C. L. Wu, J. Electrochem. Soc. **118**, 1909 (1971).
[11] I. Ekvall, E. Wahlström, D. Claesson, H. Olin, and E. Olsson, Meas. Sci. Technol. **10**, 11 (1999).
[12] Y. Nakamura, Y. Mera, and K. Maeda, Rev. Sci. Instrum. **70**, 3373 (1999).
[13] L. Anwei, H. Xiaotang, L. Wenhui, and J. Guijun, Rev. Sci. Instrum. **68**, 3811 (1997).
[14] A.-D. Muller, F. Muller, M. Hietschold, F. Demming, J. Jersch, and K. Dickmann, Rev. Sci. Instrum. **70**, 3970 (1999).
[15] L. Ottaviano, L. Lozzi, and S. Santucci, Rev. Sci. Instrum. **74**, 3368 (2003).
[16] V. T. Binh and R. Uzan, Surf. Sci. **179**, 540 (1987).
[17] L. N. R. H. Fowler, Proc. R. Soc. London, Ser. A **119**, 173 (1928).
[18] T. T. Tsong, *Atom-Probe Field Ion Microscopy* (Cambridge University Press, Cambridge, England, 1990).
[19] H. W. Fink, IBM J. Res. Dev. **30**, 460 (1986).
[20] E. W. Muller, J. Appl. Phys. **27**, 474 (1956).
[21] E. W. Müller and T. T. Tsong, *Field Ion Microscopy Principles and Applications* (Elsevier, New York, 1969).
[22] A. Moore, J. Phys. Chem. Solids **23**, 907 (1962).
[23] M. Rezeq, J. Pitters, and R. Wolkow, J. Chem. Phys. **124**, 204716 (2006).
[24] H.-S. Kuo, I.-S. Hwang, T.-Y. Fu, J.-Y. Wu, C.-C. Chang, and T. T. Tsong, Nano Lett. **4**, 2379 (2004).
[25] T.-Y. Fu, Y.-R. Tzeng, and T. T. Tsong, Phys. Rev. B **54**, 5932 (1996).
[26] M. Greiner and P. Kruse, Rev. Sci. Instrum. **78**, 026104 (2007).